

Analysis of the DEMO-FNS magnetic field passive reduction and neutral beam injectors shielding methods

S.S. Ananyev^{a)}, E. D. Dlougach, A.V. Klishchenko

National Research Center «Kurchatov Institute», 1 Ak. Kurchatov sq., Moscow, 123182, Russia

^{a)} Corresponding author: Ananyev_SS@nrcki.ru

Abstract. Steady-state operation mode of a fusion neutron source (FNS) will require plasma heating and maintaining the current in it by fast atoms beam injecting. The DEMO-FNS project assumes the use of six injectors providing additional heating power up to 30 MW at an atomic energy of 500 keV. As a prototype for the DEMO-FNS injector, an injector developed in detail for the ITER project can be used, with the injector layout retained, but changes in individual components, which is caused by the difference in beam energy and power. Inside these components, there are very strict restrictions on the magnetic field magnitude (the flux density should be below a certain value along the path of ion movement and even lower in the neutralization region). To achieve these characteristics in an environment with a high scattered field due to the magnetic system of the facility, which includes the coils of the poloidal and toroidal fields, the central solenoid and the plasma itself, additional shielding of the injectors is provided. At this stage, we expect that the proposed design will allow obtaining the required magnetic field values only by passive injector(s) shielding due to a case made of a ferromagnetic material with a high magnetic permeability index. An electromagnetic analysis of the effectiveness of such a screen was performed using 3D modeling using the ANSYS code. The BTR code was used to loads calculation along the entire injection path length in the obtained magnetic fields conditions, taking into account a reionization.

INTRODUCTION

In the DEMO-FNS project [1-3] (calculated for a fusion power of 40 MW and based on a tokamak with a large radius of 3.2 m, a small radius of 1 m, an elongation of the plasma 2 and superconducting coils that create a field on the axis of the plasma column of 5 T) it is proposed to use six (in accordance with the vacuum chamber sectors number) [4] heating injectors as part of the neutral beam injection system (NBIs) [5]. NBI DEMO-FNS should provide the possibility of steady-state plasma heating and current generation in core, due to the sequential injectors operation mode, with considering the injector cryopanel warming mode (to extract the gas accumulated on them) and their scheduled service.

As was discussed in detail in [5 and 6], for efficient beam transportation in a neutral beam injection system, it is necessary to reduce the scattered magnetic field of the facility (due to the effect of plasma and the DEMO-FNS magnetic system) inside the beamline elements. For this, both passive decrease methods and active ones with the use of additional magnetic field coils can be used [7].

In this work, we analyzed the ways to provide working conditions (in terms of the magnetic field) for heating injectors and made an assessment of the loads on the injection path components arising from direct particle interception and reionization. The stray magnetic fields calculation in the injectors area was performed using the ANSYS code. To assess the loads the codes PDP [7], BTR [8] and the obtained magnetic field profiles, as well as the gas density profile calculated by the MCGF code [9], were used.

REQUIREMENTS FOR THE SYSTEM FOR REDUCTION THE MAGNETIC FIELD IN THE INJECTOR

Requirements for the magnetic field decrease system for NBI DEMO-FNS were obtained in the beamline optimization calculations process, performed earlier in [5, 6]. The critical values for the magnetic induction component are summarized in Table 1 for various injector elements. The most stringent condition for the admissible field value $B_z < 1$ G refers to the region from the exit from the ion accelerator to the neutralizer and in it, since charged particles are subject to deflection under the magnetic field influence. After neutralization, particles are less susceptible to deflection in a magnetic field, therefore in the area between the neutralizer output and the RID input the requirements for the field value are lower. The field magnitude in the region of the calorimeter and the gap between it and the scraper - the element at the outlet from the injector, is an order of magnitude lower than the critical value in the neutralizer. Requirements for the magnetic field magnitude in the duct are not established, since it ensures the reionized particles deflection throughout the entire beamline length, reducing the power density on the duct walls. Since the magnetic field profiles have a rather flat shape in the injector region, the requirements for the shielding system dictate the minimum value of all.

In [6], the change in the neutralization efficiency and beam transport was shown depending on the vertical magnetic field magnitude (in the section from the ion source to the RID). Calculations were performed for perfect focusing in the selected two-channel geometry. It is desirable to ensure that the stated conditions are met with a certain margin, which will ensure the predicted mode and beamline efficiency.

TABLE 1. Residual magnetic field requirements for different injector elements. X is the distance measured from the ion source in the plasma direction - to the point where the beam touches the plasma surface, Y is the horizontal coordinate perpendicular to X, and Z is the vertical coordinate coinciding with the tokamak symmetry axis.

Region	Xmin (m)	Xmax (m)	Ymin (m)	Ymax (m)	Zmin (m)	Zmax (m)	Requirement on B (G)
Scraper	8.5	9.5	3.0	4.0	-1	0	<10
RID	4.5	6.5	3.0	4.0	-1.25	0.25	<10
Neutralizer	1.5	4	3.0	4.0	-1.25	0.25	<1
Gap	1	1.5	3.0	4.0	-1	0	<1
Beam source	-1	0	3.0	4.0	-1	0	<10

DEMO-FNS FACILITY MODEL FOR THE MAGNETIC FIELD CALCULATION

The NBI injector case is located at a considerable distance from the magnetic system (the length of the beam line is > 20 m). In this area, the greatest influence is exerted by the magnetic field formed by poloidal coils, however, we consider it important to take into account all sources for a correct calculation: poloidal coils, toroidal coils, central solenoid and plasma. We have created a computational finite element model, which includes an expanded vacuum volume in which the DEMO-FNS electromagnetic system is located. Figure 1 shows the DEMO-FNS finite element computational model with an injector magnetic shield. The vertical diametrical section of the complete DEMO-FNS electromagnetic model is shown in Figure 2. The currents values in 18 toroidal, 8 poloidal coils, 6 central solenoid sections and in the plasma used in the calculations are presented in Table 2. Since the injection axis in this model is not oriented axisymmetrically in the facility cylindrical coordinate system parallel to both the tangent to the plasma core and the facility vacuum chamber equatorial plane, we considered not a compact axisymmetric sectoral model, but a complete finite element model of the entire facility, which includes currents in all coils and plasma and an exact three-dimensional geometry of the injector relative to the facility location.

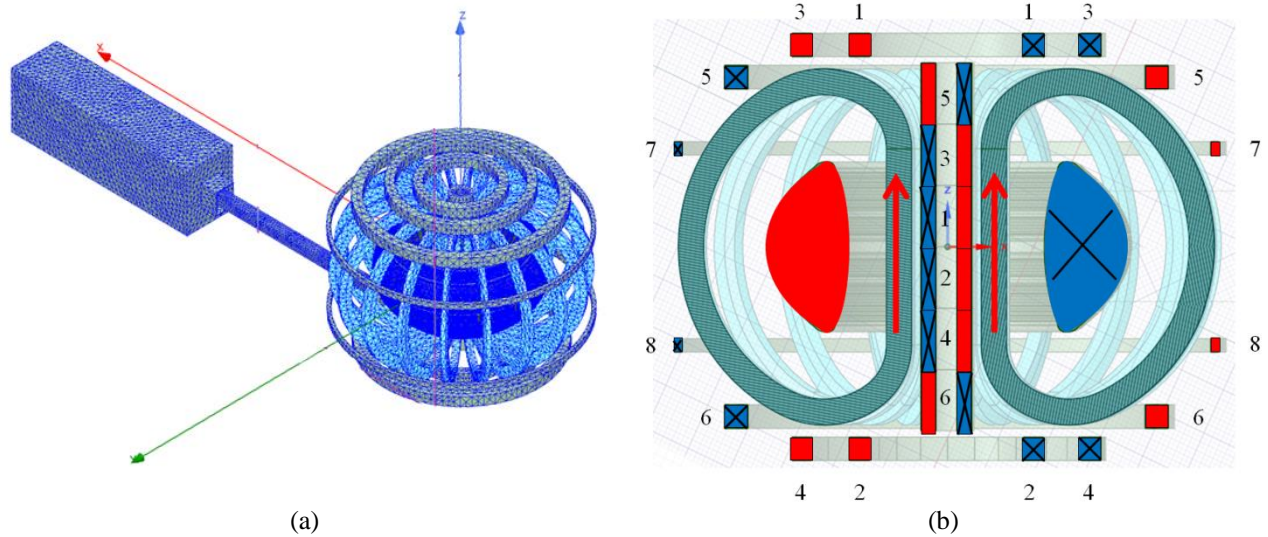


FIGURE 1. DEMO-FNS finite element computational model with an injector magnetic shield (a). Vertical diametrical section of the DEMO-FNS complete electromagnetic model (b). The magnetic system elements are shown, in which currents are taken into account when calculating the resulting magnetic fields: toroidal and poloidal coils, central solenoid sections and plasma. The colors show the coils and the current directions in them (with a cross - the current "from us"). The current direction in the toroidal coils is indicated by arrows. The coil numbers correspond to the designations in Table 2.

TABLE 2. Current values in 18 toroidal and 8 poloidal coils, 6 central solenoid sections and in plasma.

Coils	Current (kA)
Toroidal coil №1-18	4300
Poloidal coil №1	8026
Poloidal coil №2	8026
Poloidal coil №3	6105
Poloidal coil №4	6105
Poloidal coil №5	5881
Poloidal coil №6	5881
Poloidal coil №7	1360
Poloidal coil №8	1360
Plasma	5000
Solenoid – section № 1	11509
Solenoid – section № 2	11509
Solenoid – section № 3	2148
Solenoid – section № 4	2148
Solenoid – section № 5	965.7
Solenoid – section № 6	965.7

CONSIDERATION OF DIFFERENT MF REDUCING METHODS TO PERMISSIBLE LEVEL AND SHIELDING SCHEME SELECTION

First, we calculated the magnetic induction components magnitude on the injection axis without shielding the injector region. Figure 3 shows the three components B_x , B_y , B_z dependences on the X coordinate (in the facility coordinates, the distance is counted from the poloidal plasma section, to which the injection axis is perpendicular). For clarity, the field components values are given on different scales: in the area of the facility magnetic system, where the characteristic fields values are T units, and the area outside it, where the all field components values do not exceed 0.05 T. It can be seen that the vertical magnetic induction component B_z in the interest to us region (the

injector region) is maximum and varies from 300 G at the input (from the torus side) to 150 G at the other end of shielding case. The Bx component changes from 20 to 2 G. The By component has the smallest values its value is about 1/4 of the value of the Bx component. Thus, Bz is the determining magnetic induction component for the injection path operation. Calculations also show an extremely insignificant effect of the central solenoid coils currents on the total magnetic field in the injector area. However, the design model includes the central solenoid coils currents.

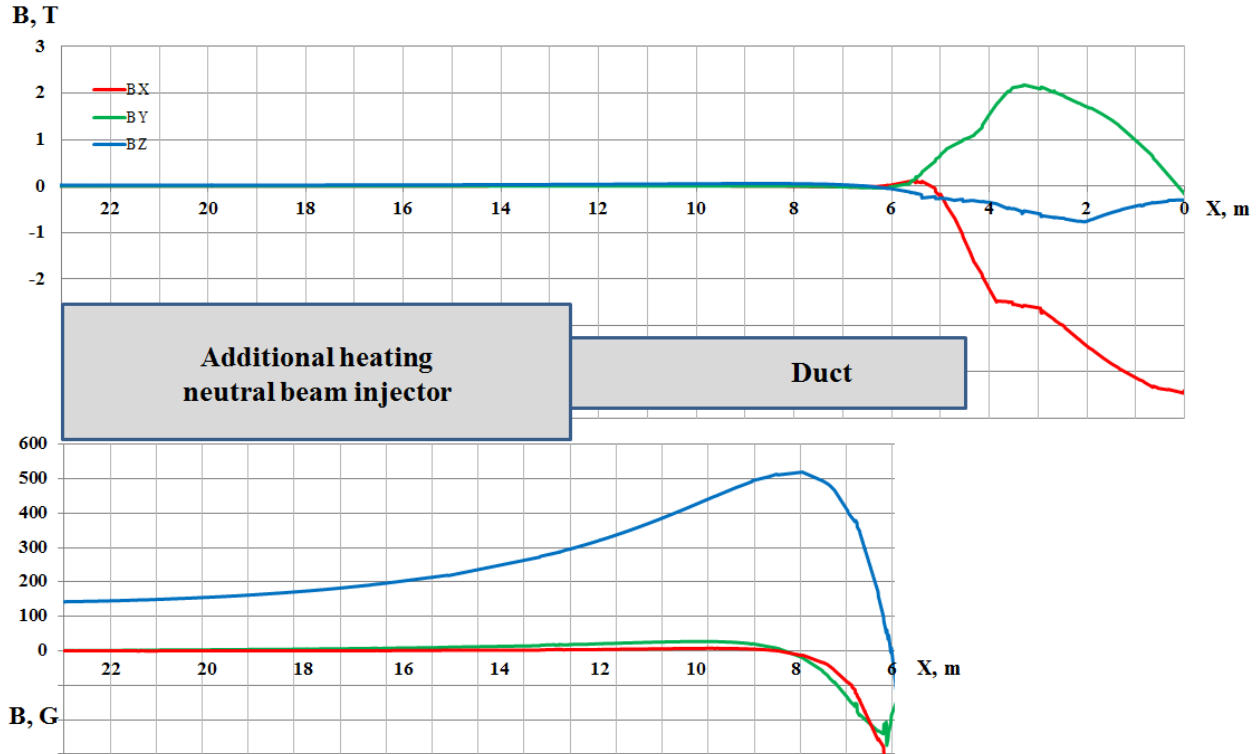


FIGURE 2. Dependences of three components Bx, By, Bz - the magnetic induction vector projections on the plane perpendicular to the beam direction, on the distance X. The distance X is counted relative to the injector ion source position. For clarity, the MF components values are given on different scales: in T (top) and G (bottom). The injector case and the duct are conventionally shown.

Optimizing of passive magnetic shielding

To carry out the calculations, a injector magnetic screen model was created - a multilayer case with external dimensions of $11.5 \text{ m} \times 3.5 \text{ m} \times 3 \text{ m}$ from a material with high relative magnetic permeability and variable layers thickness, vacuum gaps between them and their number. Thus, a passive screen is a set of nested boxes with the same wall thickness with certain vacuum gaps between successively nested boxes, by analogy with a "nesting doll".

The magnetic shield optimization was carried out in order to effectively suppress the magnetic field inside the injector case to reduce losses in the beamline. As already noted, at this stage we did not consider the elements of active magnetic field suppression, limiting ourselves to passive protection. In contrast to the decision made in ITER, where ferromagnetic steel 15 cm thick is used as the screen material (in combination with 7 active magnetic field suppression coils), we are considering the possibility of making the injector case from permalloy or electrical steel. The paper considers a precision magnetic soft alloy 50H. This alloy has an increased magnetic permeability and technical saturation increased induction at least 1.5 T, belongs to the permalloy category, iron-nickel alloys with increased permeability values in weak fields conditions. Alloy 50H contains 40-50% nickel. According to open information, sheets up to 800 mm wide and up to 32 mm thick are manufactured by agreement between the consumer and the manufacturer. In the calculations, the initial relative magnetic alloy permeability was taken to be constant equal to 5000, independent of the magnetic induction value in the given magnetic shield material due to the low magnetic field values in the computational domain.

We have considered options for single-layer shielding with a thickness of 5 cm, as well as two-, three- and four-layer with different layer thicknesses and various vacuum gaps between them. A calculations series was performed to select the optimal layer thicknesses and vacuum gaps between layers for optimal passive suppression of the magnetic induction vector projection on planes perpendicular to the beam direction. As already noted, the main criterion is the field value in the region from the ion source and in the neutralizer, which should not exceed 1 G. Figure 4 shows graphs of the maximum magnetic field component B_z , depending on the magnetic shield layers number and the used shield material relative magnetic permeability values. The field profiles in the figure are shown to scale with the injector case and the components inside - you can see which injection path area corresponds to certain the residual field values.

The most suitable options turned out to be a single-layer with a 5 cm thickness and a relative magnetic permeability equal to 15000, two-layer with a layer 2.5 cm thickness and a relative magnetic permeability equal to 10,000, and a four-layer with 2.5 cm layers and a relative magnetic permeability equal to 5000. In this case, the requirements for the magnetic field magnitude in the most critical injector region - the neutralizer and the ion source are satisfied only by the last option and partially by the first.

The calculations showed that by increasing the screen layers number made of a material with a lower relative magnetic permeability value, it is possible to achieve better screening than when using one layer of material with a larger relative magnetic permeability value with the same total thickness. As a result, we did not consider other options for using permalloy with relative magnetic permeability of 10,000 and 15,000, since these materials are expensive and the manufacture of thick-walled multi-ton structures may not be technologically feasible.

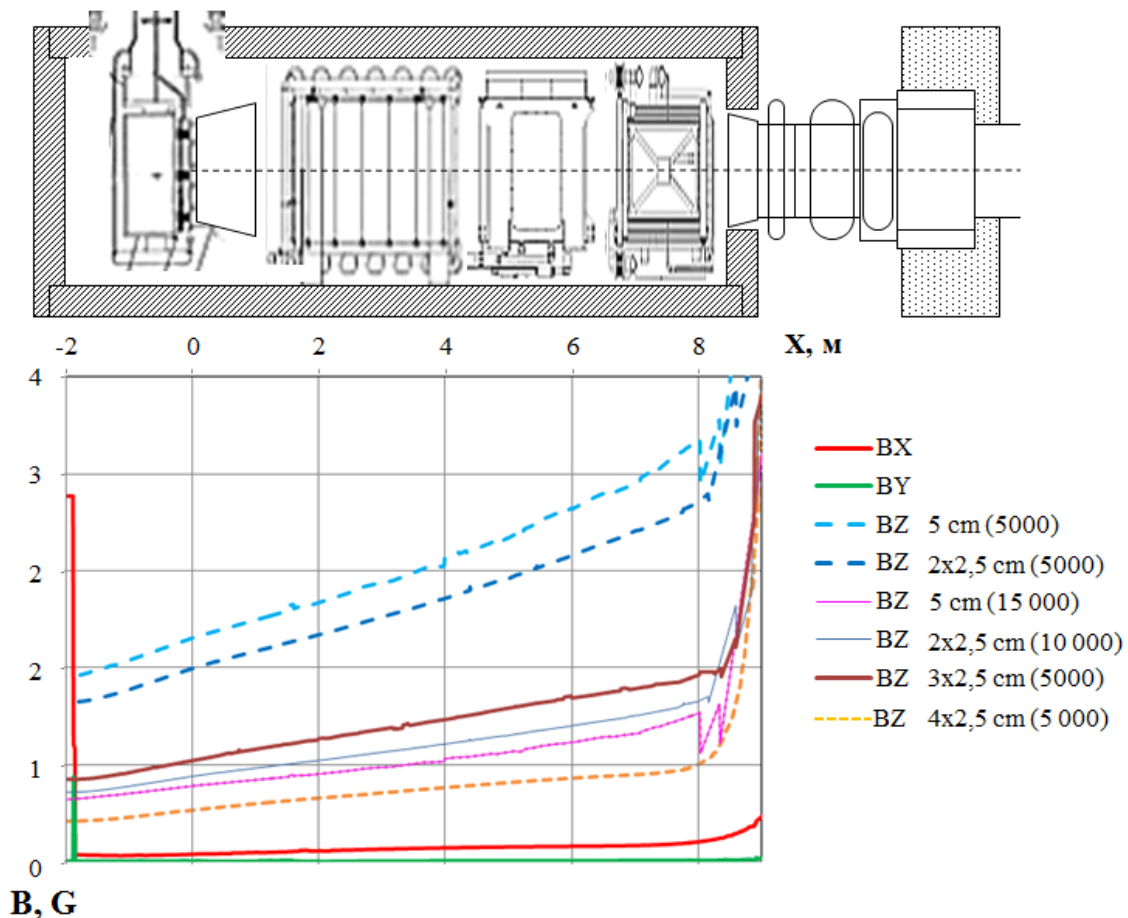


FIGURE 3. Residual field from the B_z component on the beam axis in the injector case area for different screen options: with different layer thicknesses and relative permeability index. Top to scale shows injector case scheme with components inside.

ASSESSMENT OF LOADS ON INJECTION TRACT COMPONENTS AND PASSING POWER UNDER MAGNETIC FIELDS

For the calculated shielded magnetic field profile in the injector corresponding to the design of a four-layer (25 mm each) magnetic shield 50H permalloy made with a relative magnetic permeability 5000 and vacuum gaps between them 10 mm, the particle motion was calculated under the obtained magnetic fields conditions, taking into account reionization with applying the BTR code.

The ion trajectories and the corresponding heat loads distribution are determined by the magnetic field configuration. Ions deflection released from the source until they are neutralized, i.e. in the section from the source to the neutralizer outlet can lead to incomplete residual ions interception in the ion receiver (RID). The magnetic field distorts the internal angular beamlets distribution. The calculations used the magnetic field values in different beamline parts (see Table 1) and the magnetic field profiles obtained as a result of passive magnetic protection optimization.

Loads distribution and power losses on injector components calculations

Table 3 shows the data on the loads distribution and power losses on the injector components and the transverse beam power dynamics obtained using the BTR code. The last column gives data for the worst case - when the magnetic field direction causing the particles coincides deflection with the beam axis deflection due to inaccurate focusing.

Calculations have shown that, for a given magnetic field distribution, the loads on the duct are significantly uneven - despite the fact that the peak load falls on one wall, the total load on the other is twice as high. Irregularity and reionized particles streams focusing in magnetic fields are the most dangerous from the heat removal point of view.

TABLE 3. Changes in the beam power along the injection track and the distribution of the loads and peak power densities between its components. The beam power at the ion source exit is 20 MW. The beam divergence is 7 mrad and the halo radiation divergence is 30 mrad. The last column takes into account the magnetic field (MF) influence.

The horizontal deflection is -2mrad - so that the effects of deflection and magnetic field (MF) add up and not compensate (worst case).

The angle of horizontal/vertical deflection of the beam axis, mrad	0/0	2/4	-2/4 (+MF)
Beam load power in the neutralizer, MW	1.18	1.25	1.24
Peak power density at the end elements of the neutralizer, MW/m ²	1.4	1.9	1.75
Peak power density on the neutralizer channel wall, MW/m ²	0.16	0.21	0.26
Neutral beam power at the neutralizer exit, MW	11.29	11.25	11.13
Neutral beam power loss inside the RID, MW	0.63	0.69	0.77
Total power released in the RID (atoms + ions), MW	8.16	8.19	8.6
Peak power density on the exposed edge of the RID panel, MW/m ²	2.6	3.30	4.8
Peak power density on the RID panel, MW/m ²	3.7	4.0	4.4
Neutral beam power at the RID exit, MW	10.67	10.56	10.0
Peak power density on the calorimeter panel, MW/m ²	11.25	11.25	11.0
The beam power intercepted by the scraper, MW	0.105	0.12	0.22
Peak power density on the scraper wall, MW/m ²	0.14	0.26	0.53
Beam load power on the walls of the duct liner, MW	0.83	1.0	1.64
Peak power density on the side wall of the liner, MW/m ²	0.21	0.37	0.73
Peak power density on the upper wall of the liner, MW/m ²	0.1	0.38	0.54
Neutral beam power introduced into the plasma, MW:			
- excluding losses due to reionization	9.73	9.43	9
- with allowance for the 10%-losses due to reionization	8.76	8.49	8.02

CONCLUSION

A computational finite element model DEMO-FNS was created, which includes a vacuum volume in which an electromagnetic system is located and one of 6 heating injectors. The magnetic field induction components values on the injection axis are calculated without screening the injector region. It was shown that without magnetic shielding, the vertical field component B_z in the injector region is maximum and is in the range of 300 G at the input (from the facility side) to 150 G in the ion source region. The magnetic shield calculations were performed on the basis of the requirements for the magnetic field values in the injector obtained by the authors earlier. At this stage, we expect that the proposed design will allow obtaining the required magnetic field values by passively shielding the injector (s) by means a case made of a ferromagnetic material with high magnetic permeability.

Variants of single-layer shielding using various materials and multilayer ones were considered: two-, three- and four-layer with different layer thicknesses and vacuum gaps between them. By choosing the optimal layers thicknesses and vacuum gaps between them, the magnetic field suppression in the injector components region was obtained to acceptable values. As a calculations result the four-layer magnetic injector shield design with a layer 25 mm thickness of and 10 mm vacuum gaps was chosen. The electrical steel using possibility with a relative magnetic permeability 4000 as a magnetic shield material is considered - its use eliminates the permalloys disadvantages, such as changes in magnetic properties during deformations and difficulties associated with welding. This could be the further modeling subject.

The loads distributions and power losses on the injector components and the transverse beam power dynamics are obtained. Loads calculations showed that for a given magnetic field distribution, the loads on the duct are significantly uneven - despite the fact that the peak load falls on one wall, the total load on the other is twice as high. Irregularity and reionized particles streams focusing in magnetic fields are the most dangerous from the heat removal point of view.

ACKNOWLEDGMENTS

The authors are grateful to A.A. Panasenkov for advice and assistance in writing this article. This work was supported by the National Research Center "Kurchatov Institute" (14.08.2019 № 1805).

REFERENCES

1. B.V. Kuteev, P.R. Goncharov, V.Yu. Sergeev, V.I. Khripunov "Intense fusion neutron sources", Plasma Phys. Rep., 2010, vol. 36, p. 281.
2. B.V. Kuteev, E.A. Azizov, P.N. Alexeev, V.V. Ignatiev, S.A. Subbotin, V.F. Tsibulskiy "Development of DEMO-FNS tokamak for fusion and hybrid technologies", Nucl. Fusion, 2015, vol. 55, p. 073035; doi:10.1088/0029-5515/55/7/073035.
3. Y. S. Shpanskiy, "Progress in the design of the DEMO-FNS hybrid facility," Nucl. Fusion, vol. 59, no. 7, p. 076014, Jul. 2019.
4. E.A. Azizov, S.S. Ananyev, V.A. Belyakov et al. "Tokamak DEMO-FNS: concept of magnet system and vacuum chamber", Physics of Atomic Nuclei, 2016, vol. 79, № 7, p. 1125—1136.
5. S.S. Ananyev, E.D. Dlougach, A.I. Krylov, A. A.Panasenkov and B. V. Kuteev "Concept of Plasma Heating and Current Drive Neutral Beam System for Fusion Neutron Source DEMO-FNS", Physics of Atomic Nuclei, 2019, Vol. 82, No. 7, pp. 981–990, DOI: 10.1134/S1063778819070020.
6. S.S. Ananyev, E. D. Dlougach, B.V. Kuteev, A.A. Panasenkov "Modelling and optimization of neutral beam injectors for fusion neutron source DEMO-FNS" - VANT. Ser. Fusion, 2018, vol. 41, no. 3, DOI: 10.21517 / 0202-3822-2018-41-3-57-79.
7. ITER Final Design Report, DDD 5.3, 2001
8. BTR website: <https://sites.google.com/site/btrcode/>.
9. A.I. Krylov and R. S. Hemsworth "Gas flow and related beam losses in the ITER neutral beam injector", Fusion Eng. and Des., 2006, vol. 81, Issue 19, pp. 2239-2248.